BOLLETTINO DI GEOFISICA TEORICA ED APPLICATA VOL. 38, N. 3-4, pp. 211-228; SEP.-DEC. 1997

Geomagnetic time variations and high definition study of space magnetic effects induced by artificial submerged sources

O. FAGGIONI [1], [2], N. BEVERINI [1], [3] and C. CARMISCIANO [1]

[1] *Istituto di Geofisica e Ambiente Marino, Consorzio Universitario di La Spezia - Università di Pisa, La Spezia, Italy*

[2] *Dipartimento di Scienze della Terra, Università di Pisa, Italy*

[3] *Dipartimento di Fisica, Università di Pisa, and INFM Pisa, Italy*

(Received November 11, 1994; accepted February 2, 1997)

Abstract. We describe a technique for high definition marine coastal survey in which we have used to locate possible artificial magnetic sources, such as wrecks, in the Eastern Ligurian Sea. The data were recorded with a marine proton magnetometer using a high density grid. The accuracy in grid location was measured by a network of three coastal position stations, transmitting in 5.48 GHz band. Magnetograms obtained from a geomagnetic observatory, located in a magnetically quiet area on the Isle of Tino, less than, 0.5 km from the east edge of the survey area, were used for the time reduction of the marine survey data. By this method the crossover errors were reduced to the instrumental accuracy level (1 nT). The local magnetic anomaly due to a source on the sea bottom (at about 35-70 m depth in the explored area) can be deduced from the high frequency component of the spectral analysis of the corrected and reduced to the pole data. A map of the field derivative was calculated. The result evidences a signal from a possible small artificial source, equivalent to several tons of iron, at a location where a subsequent submarine exploration demonstrated the presence of a small wreck.

1. Introduction

During the last few decades, marine magnetic survey techniques have contributed significantly to general crustal studies and to mining and environmental research.

As far as regional research is concerned, the problems involved in obtaining detailed data was solved in the early 1970s, when extremely accurate mappings of large oceanic areas were produced (Vogt and Avery, 1974; Guennoc et al., 1979; Roberts et al., 1985; Verhoef et al., 1991;

Corresponding author: O. Faggioni; Ist. Geofisica e Ambiente Marino, Consorzio Universitario di La Spezia - Università di Pisa, Via Fontevivo 25, 19125 La Spezia, Italy

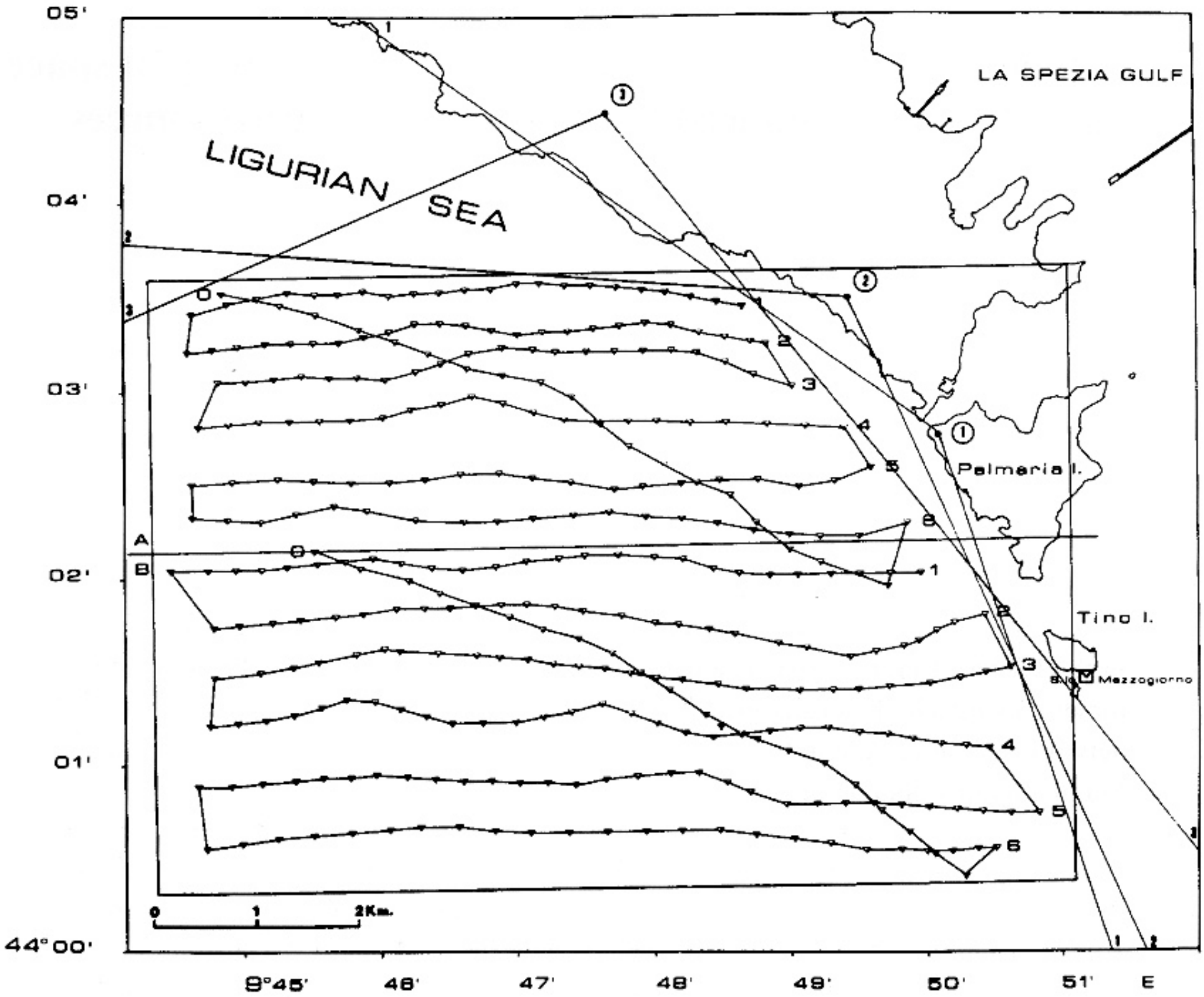

Fig. 1 - Survey map. Profiles from 1 to 6, sector A (1994JD76), and from 1 to 6, sector B (1994JD83) indicate the ship's tracks; parallel 44° 02'13" indicates the borderline between the two serveyed areas; the triangles indicate the position of the measurement points; profiles 0(A) and 0 (B) were used to assess the crossover error. Circled numbers 1, 2, and 3 indicate the transmitting stations of the coastal orientation network; the coverage angle of the surveyed area lies between the directrices 1-1, 2-2 and 3-3. The square indicates the position of the reference geomagnetic observatory installed at Spigolo di Mezzogiorno (Isle of Tino). The internal board defines the area of study.

Roest et al., 1992; Faggioni et al., 1995). In high-detailed studies of local areas, as in mineral exploration and, in particular, in environmental search for artificial submarine iron sources, the use of higher definition measurement techniques is necessary. For these, a high-definition assessment of the crossover error and an accurate positioning of the measurement point are of primary importance. These parameters are directly connected with the short-wavelength fields, and thus with the presence of possible surface magnetic sources (Talwani et al., 1971).

The availability of coastal sea navigation positioning systems, based on microwave coastal transponder systems or on differential satellite positioning systems (DGPS), allows one to achieve a spatial accuracy of about 1-3 m, under favorable weather conditions, and when using adequate vessels.

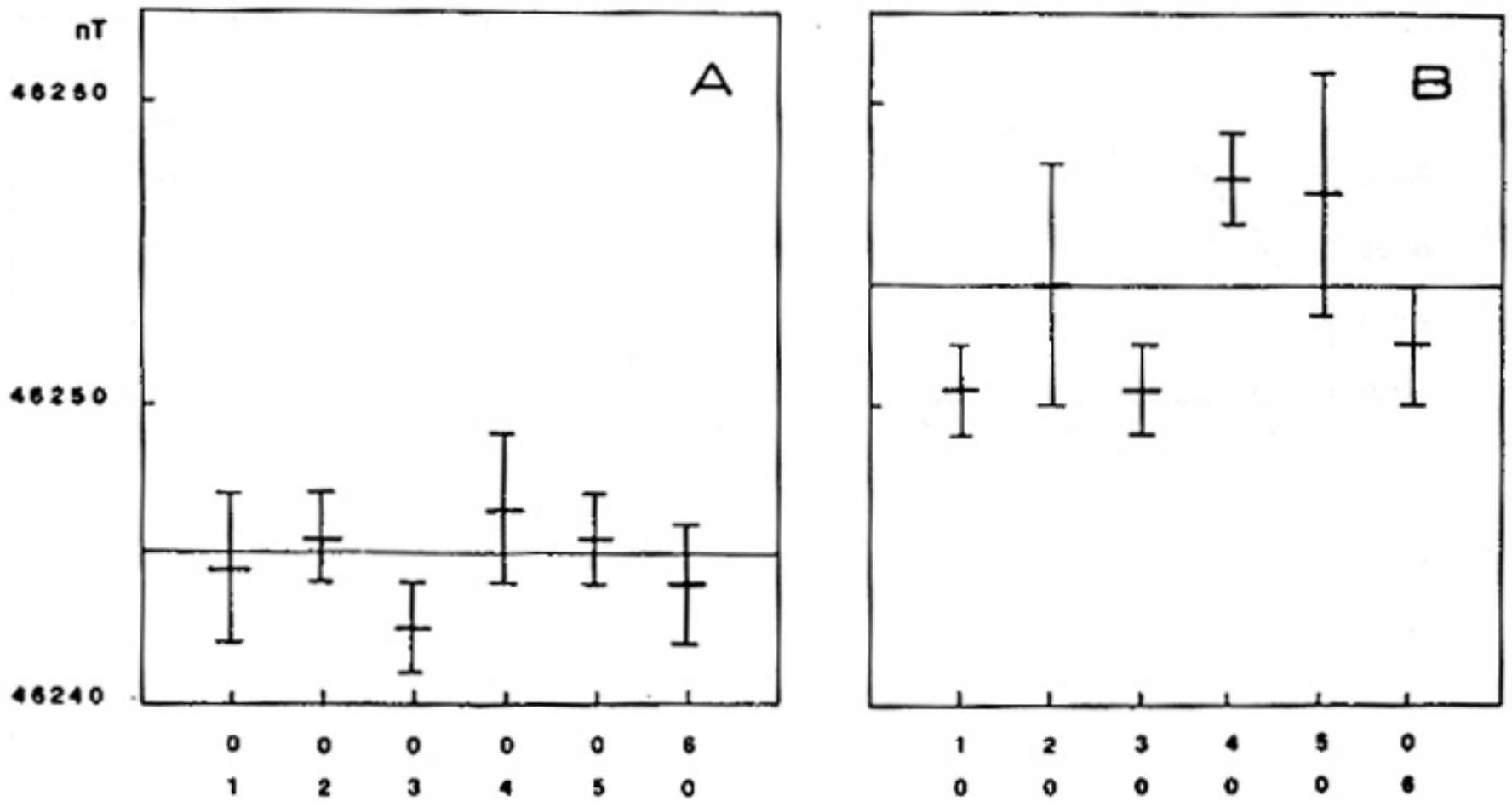

Fig. 2 - Crossover error of the observed field (not temporally reduced) assessment of the measurement differences at cross points of the observed field F in nT. A) Cross point between the measurements of 1994JD76 A1 ... A6 (abscissae 1 ... 6), and the measurements along AK (abiscissa 0). B) Cross point between the measurements of 1994JD83 B1 ... B6 (abscissae 1 ... 6), and the measurements along BK (abscissa 0) in A) and B) the central part of the crossover error segments indicates the mean value of the two measurements; the unbroken line indicates the mean field.

We have carried out a high-definition total geomagnetic intensity survey of the coastal sea area between 44° 00' 24"N - 44° 03' 36"N and 09° 44' 30"E - 09° 50' 49"E (Eastern Ligurian Sea - Mediterranean Sea) using these naval location techniques. The magnetograms registered at the same time in a temporary geomagnetic observatory located on the Isle of Tino, allow time reduction of the data, and produce a detailed description of the local geomagnetic field space structure related to surface magnetic sources.

2. Measurements and data

Measurements of the total intensity F of the geomagnetic field in the area between 44° 00' 24"N-44° 03' 36"N and 9° 44' 30"E-9° 50' 49"E (HDR Med Sea 94 project) were aimed at verifying the state of the coastal sea floor west of the isles of Palmaria, Tino and Tinetto (Eastern Liguria, Italy), and detecting submerged metal bodies. The study was carried out using a marine proton magnetometer with 12 approximately parallel profiles (Fig. 1). The average sampling rate along the profiles varied from a minimum of 235 m (profile A2) to a maximum of 350 m (profile B6), while the transverse distance between the profiles was between 150 m and 725 m.

The set was an irregular spaced rectangular matrix grid, of 39.5 km^2, major direction (W-E) length of 8,200 m, and sampling rate density from 725 m to 150 m. In theory this matrix could resolve geomagnetic signals with wavelengths between L_{MAX} = 4,100 m and band 1_{min} = 1,450-300 m.

The surveying operations (Fig. 1) took place on 1994JD76, from 9 10 (UT) to 15 18 (UT) to

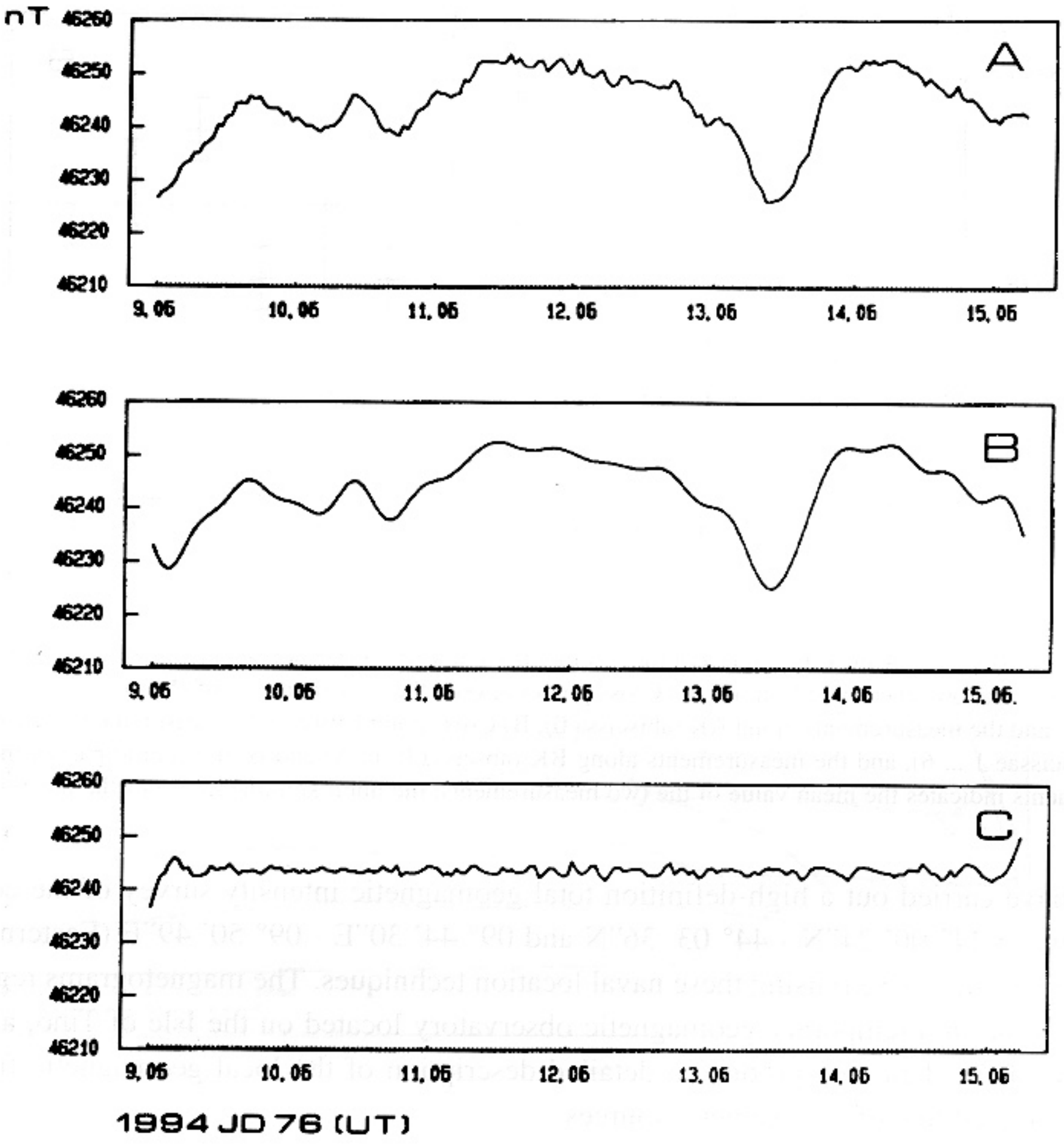

Fig. 3 - Total intensity F magnetograms of the geomagnetic field for the period 9 06 (UT): 15 20 (UT) - 1994JD76, recorded with a sampling rate of 2 min by the magnetometric station in the Isle of Tino (A); background geomagnetic signal: LP 1.6 x 10^{-3} Hz (B); local artificial noise field: HP 1.6 x 10^{-3} Hz (C).

north 44° 02' 13"N, A sector, and on 1994JD83, from 8 18 (UT) to 15 32 (UT) to south 44° 02' 13"N, B sector. On the first day the survey followed the profiles labelled in Fig. 1 A1 to A6 and the crossover test profile AK; on the second day, the profiles B1 to B6, and the crossover test profile BK.

The positioning system included a network of three transmission stations installed on the coast and on the Isle of Palmaria, and connected to a master station located onboard. Stations 1 (Isle of Palmaria; lat. 44° 02' 48.6"N, long. 9° 50' 01.7"E), 2 (Geodetic point 216; lat. 44° 03' 45.9"N, long. 9° 49' 00"E), and 3 (Campiglia; lat. 44° 04' 39.7"N, long. 9° 47' 36.4"E) formed coverage angles of respectively 144°, 118°, and 105° (Fig. 1). Each transmitting station included a position transponder at a frequency of 5.48 GHz and the power supply package. The point loca-

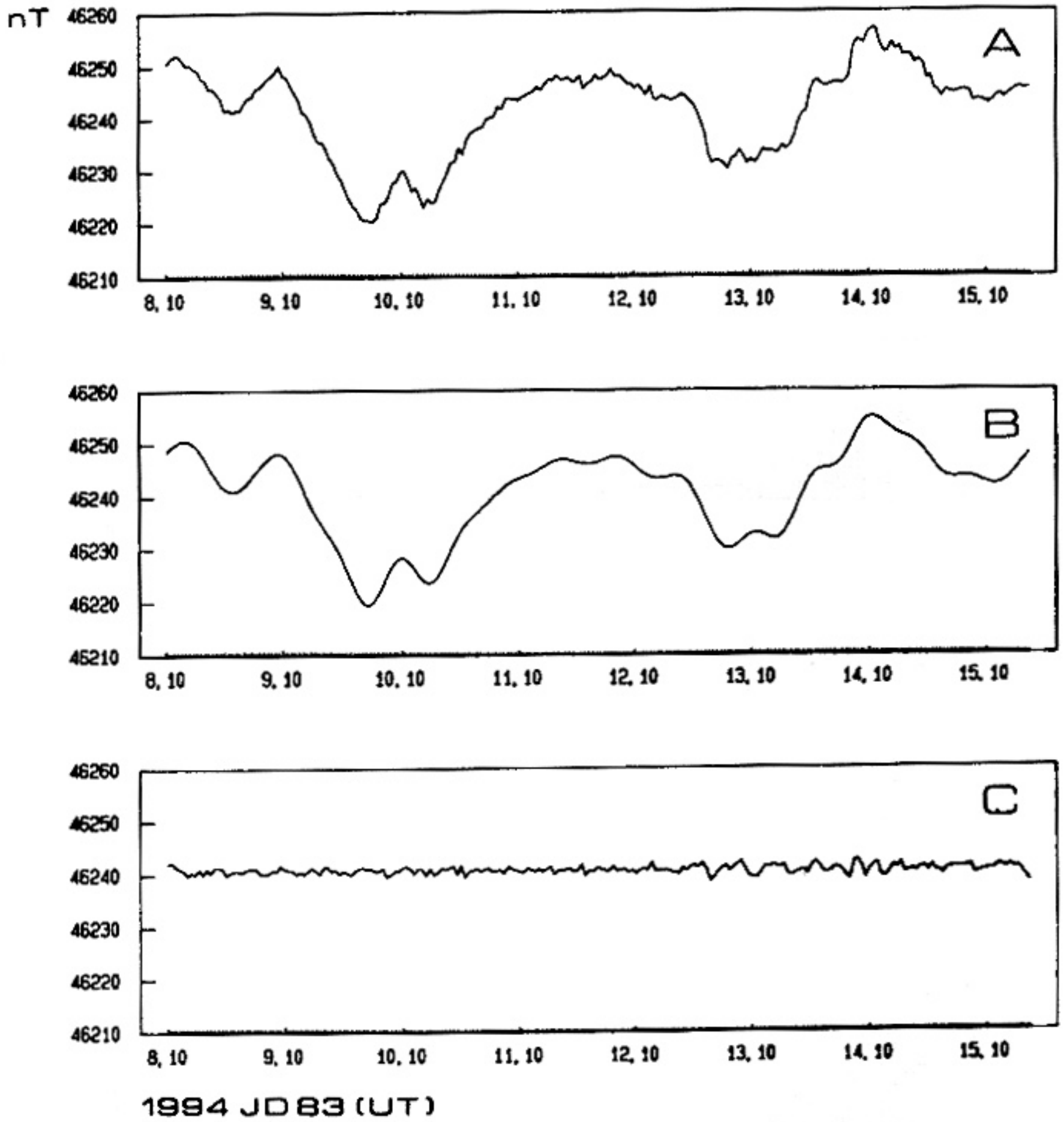

Fig. 4 - Total intensity F magnetograms of the geomagnetic field for the period 8 10 (UT): 15 32 (UT) - 1994JD83, recorded with a sampling rate of 2 min by the magnetometric station on the Isle of Tino (A); backgroundo geomagetic signal: LP 1.4 x 10^{-3} Hz (B); local artificial noise field: HP 1.4 x 10^{-3} Hz (C).

tion accuracy of the system was of the order of 2-3 m.

During the two marine surveys, a geomagnetic observatory was active at Spigolo di Mezzogiorno on the isle of Tino (lat. 44° 01' 31.8"N, long. 9° 51' 10.8"E). The magnetograms, obtained with a proton magnetometer, were used for the time reduction of the survey data (Hansen and Childs, 1987).

The two magnetometers were previously tested in the experimental observatory of the istituto di Geofisica e Ambiente Marino at Passo della Cappelletta - Varese Ligure (La Spezia) (lat. 44° 24' 03.8"N, long. 9° 39' 51.8"E) (Faggioni et al., 1993). The comparison between the two instruments from 1994JD66 was satisfactory. The differences in the reading of the geomagnetic field was below 1 nT in 94.6% of the cases, and between 1 and 2 nT in the remaining 5.3%.

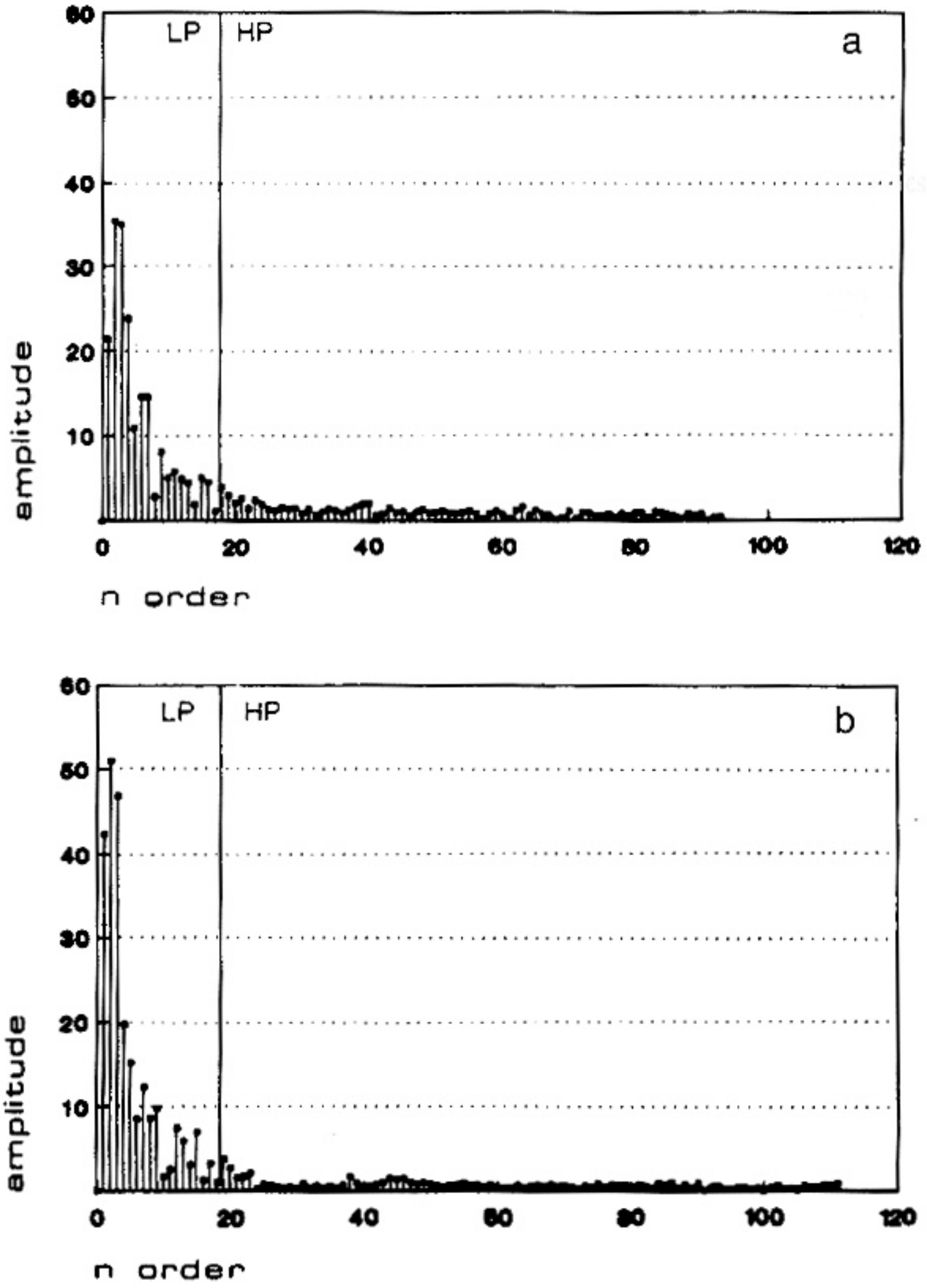

Fig. 5 - a) Amplitude spectrum of the magnetograms 9 06 (UT): 15 20 (UT) - 1994JD76. Resolution band: $F_{min} = 8.9 \times 10^{-5}$ Hz (first order), $F_{max} = 4.2 \times 10^{-3}$ Hz. Cut of frequency: 17th order. b) Amplitude spectrum of the magnetograms 8 10 (UT): 15 32 (UT) - 1994JD83. Resolution band: $F_{min} = 7.5 \times 10^{-5}$ Hz (first order), $F_{max} = 4.2 \times 10^{-3}$ Hz. Cut of frequency: 18th order.

Moreover, the biggest differences were due to magnetic field fluctuations characterized by frequencies at the highest limit of the instrumental acquisition band (3×10^{-2} Hz), not important for the time reduction of our data, because the marine surveys and the terrestrial observations at Spigolo di Mezzogiorno were carried out at a sampling rate of two minutes (4.2×10^{-3} Hz).

The time reduced technique, based on the use of a comparison between magnetograms recorded in a fixed observatory, has some advantages in comparison with the gradiometric marine survey technique. The gradiometric sensory system is more complex and heavier than the magne-

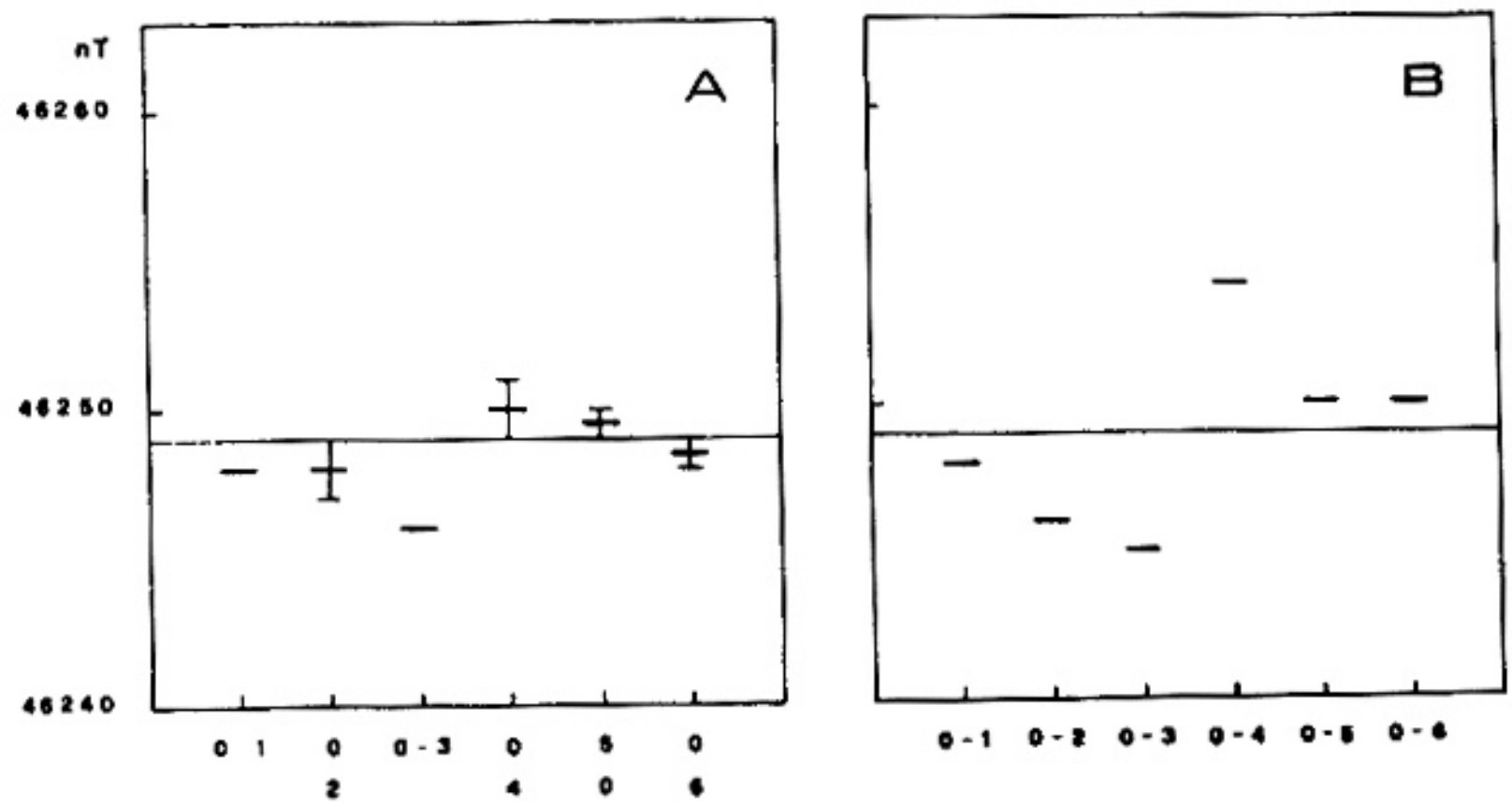

Fig. 6 - Crossover error time-reduced field. Assesment of the measurement differences of the time-reduced field. A) Cross points between the measurements of 1994JD76 A1 ... A6 (abscissae 1 ... 6), and the measurements along AK (abscissa 0). B) Cross points between the measurements of 1994JD83 B1 ... B6 (abscissae 1 ... 6), and the measurements along BK (abscissa 0). In A) and B) the central part of the crossover error segment indicates the mean value of the two measurements; the unbroken line indicates the mean field.

tometric one, and would reduce the operativity of the vessel (a GRP 12.5 m, 500 hp offshore motorboat). Furthermore, the gradiometric sensory system is considerably longer and the transverse deviation of the sensor from the track would be larger than that of the magnetometric sensor for the same ship-sensor system differential drift angle.

In our motorboat, we towed the magnetometric sensor typically at a distance of 30-50 m,

Table 1 - C.P.: cross points; φ(N), λ(E): cross points latitude and longitude (Greenwich); F(A-B): uncorrected total intensity geomagnetic field measured in the first time period [nT]; F(K) uncorrected total intensity geomagnetic field measured in the second time period [nT]; C.E.: total intensity measured F field crossover errors [nT]; T(A-B): time of first measuremente [h:min]; T(K): time of second measuremente [h:min]; ΔT: measurement time intervals [min]; *F(A-B)*: time reduced total intensity geomagnetic field measured in the first time period [nT]; *F(K)*: time reduced total intensity geomagnetic field measured in the second time period [nT]; *C.E.*: time corrected total intensity F field crossover error [nT].

C.P.	φ(N)	λ(E)	F(A-B)	F(K)	C.E.	T(A-B)	T(K)	ΔT	*F(A-B)*	*F(K)*	*C.E.*
A1 .. AK	44° 03' 34.83"	09° 44' 56.11"	46242	46247	5	09:52	15:18	326	46248	46248	0
A2 .. AK	44° 03' 22.50"	09° 45' 55.67"	46244	46247	3	10:28	15:12	284	46247	46249	2
A3 .. AK	44° 03' 10.00"	09° 46' 43.33"	46241	46244	3	11:38	15:06	208	46246	46246	0
A4 .. AK	44° 02' 51.67"	09° 47' 40.55"	46249	46244	5	12:38	14:58	140	46249	46251	2
A5 .. AK	44° 02' 32.33"	09° 48' 23.33"	46244	46247	3	13:14	14:54	100	46250	46249	1
A6 .. AK	44° 02' 18.00"	09° 48' 48.00"	46246	46242	4	14:22	14:50	28	46248	46249	1
B1 .. BK	44° 02' 06.00"	09° 45' 54.55"	46249	46252	3	08:56	15:30	394	46248	46248	0
B2 .. BK	44° 01' 53.42"	09° 46' 45.55"	46250	46258	8	09:40	15:24	344	46246	46246	0
B3 .. BK	44° 01' 31.92"	09° 47' 56.89"	46249	46252	3	11:00	15:14	254	46245	46245	0
B4 .. BK	44° 01' 09.17"	09° 48' 47.55"	46256	46259	3	12:18	15:06	168	46253	46253	0
B5 .. BK	44° 00' 47.00"	09° 49' 41.11"	46253	46261	8	12:58	14:58	120	46250	46250	0
B6 .. BK	44° 00' 31.92"	09° 50' 04.44"	46254	46250	4	14:38	14:54	16	46250	46250	0

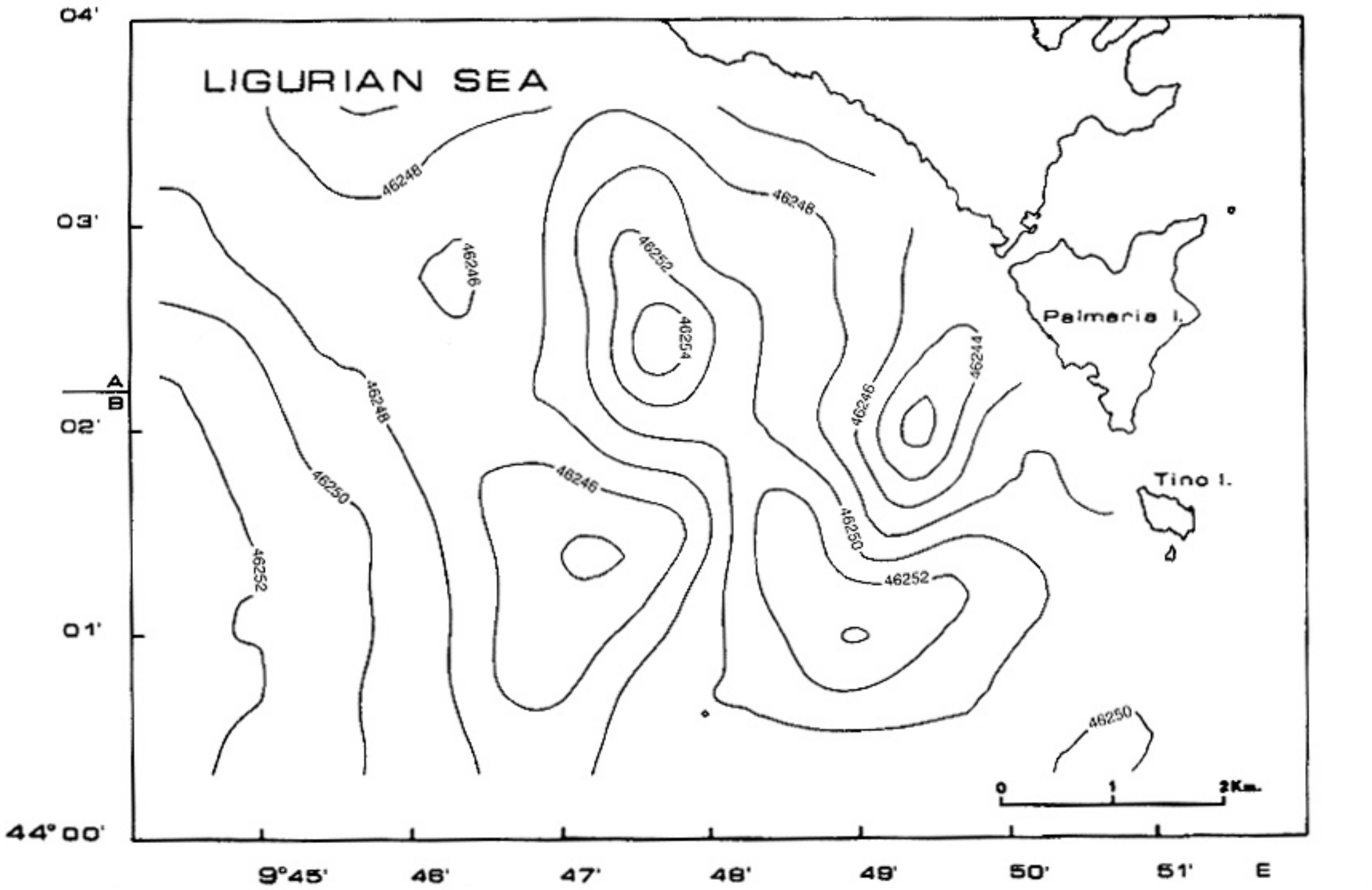

Fig. 7 - Total intensity F map reduced 15 18 (UT) 1994JD76. C.I. = 2 nT. Field variation range: 46241 ÷ 46255 nT.

while the second sensor of the gradiometric system would have been towed to a distance of 100-150 m. Thus, assuming a differential drift of 5°, the theoretical leeway of the probe, with respect to the ships track, would be between 2.6-4.3 m, within the accuracy given by the orientation system while the drift of the second sensor of the gradiometric system would be 8-13 m, reducing the accuracy by a factor 3-4. This accuracy loss, although not important in marine regional studies, is of fundamental importance in high definition surveys, when small superficial natural or artificial sources are sought.

The depth of the surveyed marine coastal area varied from a minimum of about 34 m to a maximum of about 70 m, and the sensor was dipped to a depth between 1 and 20 m. Thus, its distance from the sea floor varied from about 33 to 50 m. In the area corresponding to the most intense anomalies, the sea floor depth varied from 34 to 60 m, and thus the distance from the sensor to the sea floor was about 33 to 40 m. Such differences caused, in our case, an error of less than 1 nT, which is our instrumental sensitivity, unlike in the case of offshore regional surveys, where the altitude variatons of the sensor induced by the morphology of the sea floor are considerable (Twigt et al., 1979, 1983; Shaw et al., 1990).

3. Data editing and time reduction

The first elaboration at the measurements on JD 76 and 83, 1994 provided an irregular grid

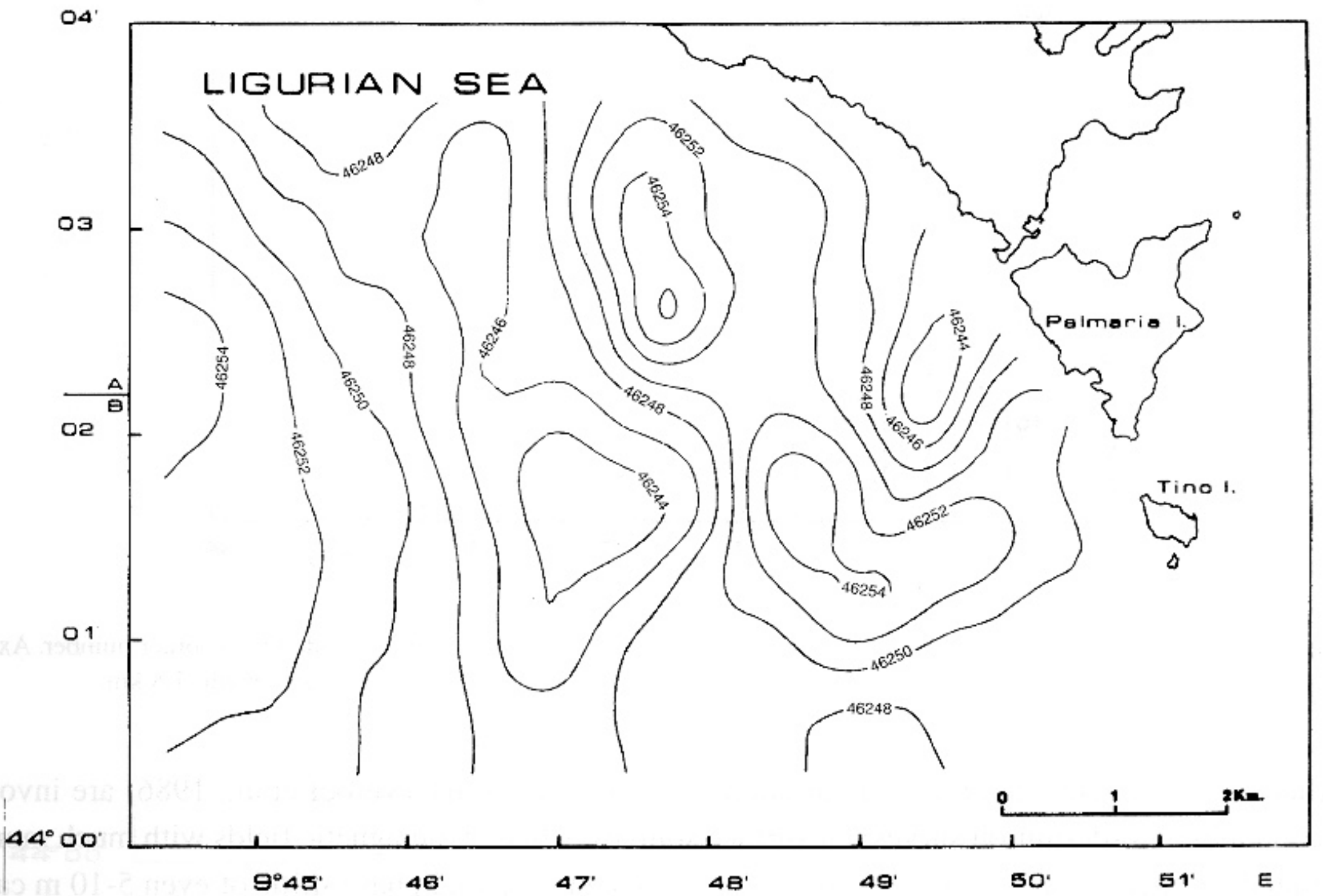

Fig. 8 - Total intensity F map reduced to the pole. C.I. = 2nT. Reduction coefficient D = 7'.20 (+) I = 60° 12'. C.I. = 2nT. Field variation range: 46243 ÷ 46257 nT.

data set which was submitted to a series of calculations in order to obtain a square grid matrix (Bott and Hutton, 1970; Harrison and Carle, 1981). The calculation area is marked in Fig. 1 by the internal perimeter. First, we defined a square grid of side l = 250 m which entirely covered the calculation area with a total of 864 points. At each point P, value F was calculated as the mean of the values measured inside a circle with center at P. The measured values were weighted proportionally to the inverse of their distance from P. The algorithm extended the radius until three measured values, or at least two values measured in nonadjacent quadrant did not fall inside the circle for every grid point. In our case, the interpolation radius vector was 490 m long. Thus, the shortest wavelength of the theoretical spectral resolution of the calculated matrix, related to the lenght of the matrix side, is 500 m.

We then calculated the difference ΔF between two successive measurements at all the crossover points, that is the points of intersection between two different ship tracks (Verhoef and Scholten, 1983; Verhoef et al., 1991). The resulting crossover errors, defined as the difference between the first field survey and the second were 3 - 8 nT (Table 1 and Fig. 2), based on 10 - 20 nT anomalies and too high for our purpose.

This crossover error has a spatial component and a time component. The spatial component is closely related to the precision of the positioning system: if it is not accurate enough, it can produce spatial phase shifts of up to hundreds of meters between the two measurements (Swan and Young, 1978). Such phase shifts have marked influence on the quality of offshore surveys,

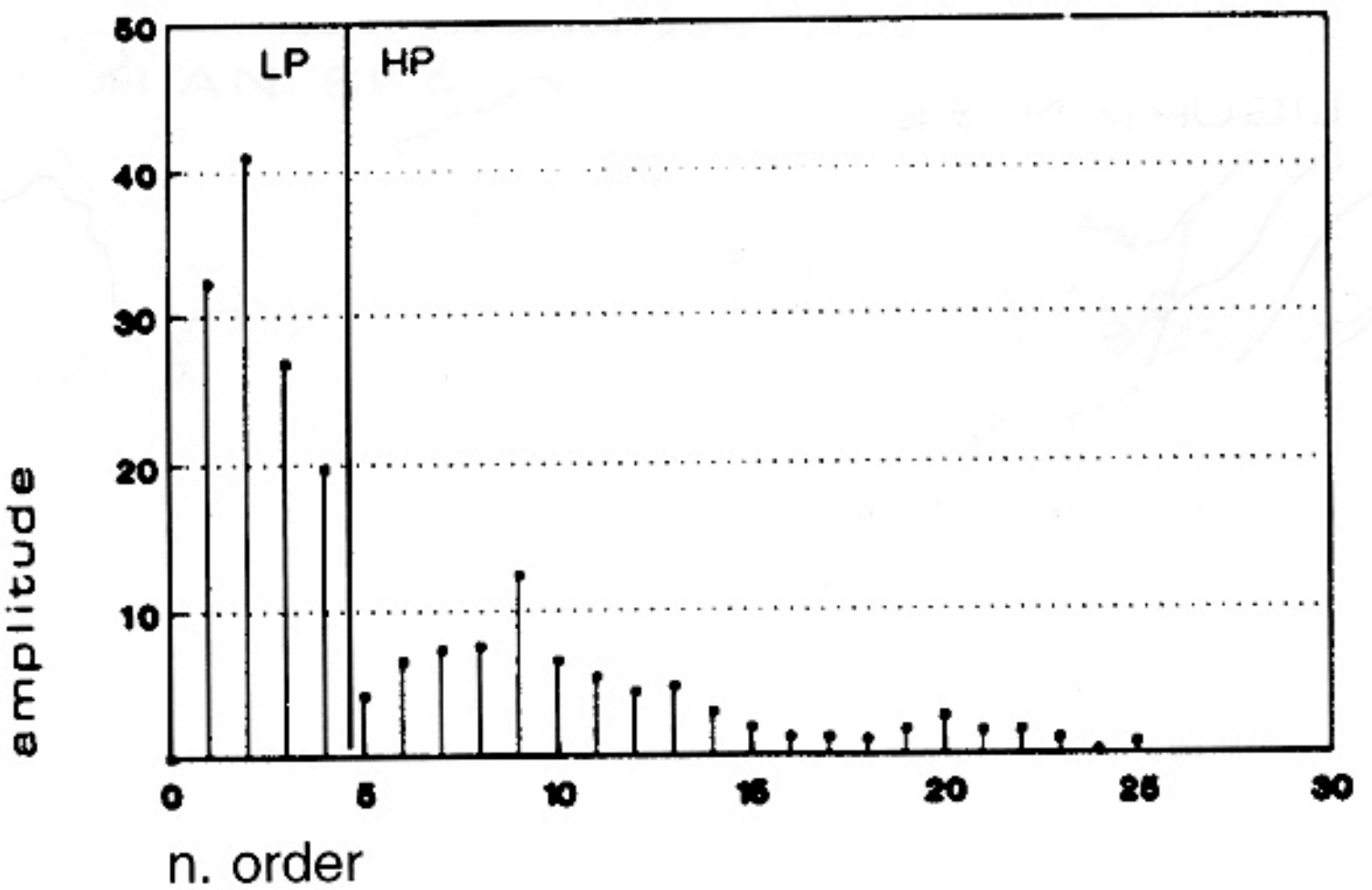

Fig. 9 - FFT amplitude spectrum of the polar-reduced total intensity F geomagnetic field. Axis x: order number. Axis y: amplitude. Matrix of calculus: 6 x 9 km; square grid side: 0.25 km. HP and LP cut wavelength: 1.8 km.

where large wavelength and field variations of some tens of nT (Veroef et al., 1986) are involved, but in high-definition surveys of surface sources, where geomagnetic fields with much more limited geometries and intensities are taken into account, spatial phase shifts of even 5-10 m can bear heavy consequences.

In our case, we had an accurate positioning system, and thus the crossover errors, measured by means of the two backsight profiles AK and BK, were essentially only time dependent. In general, the intensity F of the geomagnetic field is both a space and time function; thus two measurements, carried out at the same site but not at the same time, will inevitably yield different results. We did a temporal reduction of the measured field values by correcting the marine measurements by comparison with the geomagnetic time variations, recorded at the same time (JD 76 and 83, 1994) by the automatic observatory of Spigolo di Mezzogiorno - Isle of Tino (Figs. 3 and 4) (Meloni et al., 1984; Meloni and Palangio, 1988; Palangio and Romeo, 1988; Faggioni et al., 1991, 1993). The recording of 1994JD76 began at 9 06 (UT) and ended at 15 20 (UT); its sampling rate was 2 min for a total of 188 samples, and its FFT spectral resolution lay in a frequency band between 8.9×10^{-5} Hz and 4.2×10^{-3} Hz. The recording of 1994JD83, carried out with the same sampling rate, began at 8 10 (UT) and ended at 15 32 (UT) for a total of 222 points (frequency band between 7.5×10^{-5} Hz and 4.2×10^{-3} Hz). The two spectra show that the geomagnetic field of the recording site characterized by a local noise threshold of probably artificial origin (the electromagnetic activity of the lighthouse sited on the isle), (Bozzo et al., 1985; Berti et al., 1991; Palangio et al., 1991; De Santis, 1993). In the FFT amplitude spectra (Fig. 5), this noise is characterized by an intensity around about 2-5 nT at the highest frequencies (Cooley and Tukey, 1965).

In order to avoid transfer of this local noise into the marine surveys, we filtered the geomagnetic signals in the frequency domain. When recording 1994JD76, we carried out a LP filtering at order number 17, corresponding to a cutoff frequency of 1.6×10^{-3} Hz; in the case of 1994JD83

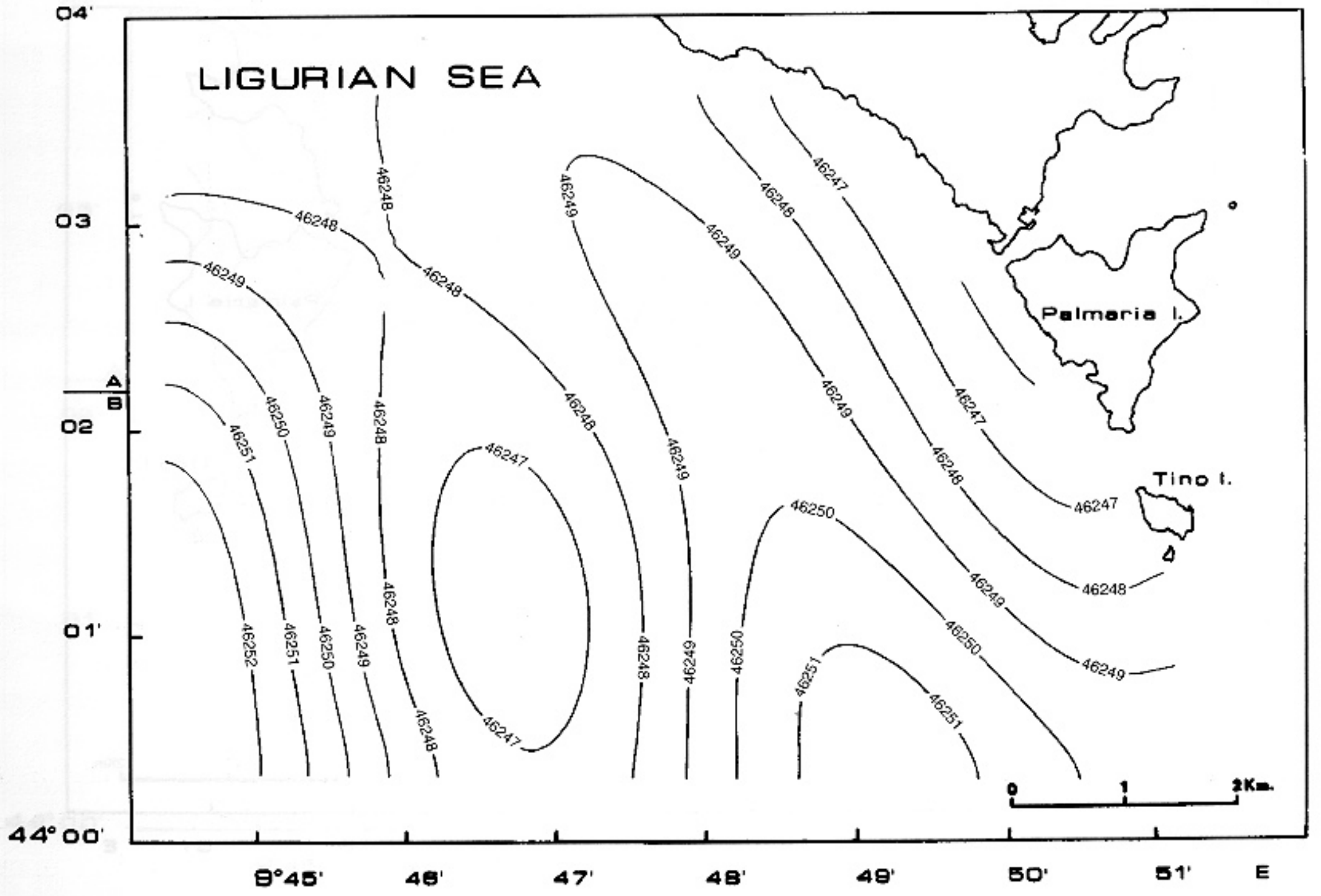

Fig. 10 - Spectral reference intensity field (SRF); low-pass filter: 1.8 km. Band of the represented harmonic components: 1.8 ÷ 4.5 km. C.I. = 2 nT.

we carried out an LP filtering at order number 18, corresponding to a cutoff frequency of 1.4×10^{-3} Hz (De Vuyst and De Meyer, 1973).

The time reduction of the entire survey was divided into two steps: first, a diurnal time reduction of each survey sector; second, reduction of the two survey sectors to the same date. To perfom the diurnal reduction we deconvolved from the field survey data at the same sampling rate (2 min) the corresponding magnetorgrams recorded by the observaotry of the Isle of Tino. The time variations are assumed constant at all points of the surveyed surface. The diurnal reduction was carried out at 15 18 (UT) of 1994JD76 in the case of survey A, and at 8 18 (UT) of 1994JD83 in the case of survey B. The two sectors of the survey were reduced to the same date by calculating the field difference recorded by the observatory between 15 18 (UT) of 1994JD76 and 8 18 (UT) of 1994JD83, and adding algebraically this difference to the reduced field B. Finally, all the samples were reduced to 15 18 (UT) of 1994JD76. Control surveys AK and BK were also time reduced.

The crossover errors of the reduced field demonstrate the effectiveness of the technique. Effectively it is lower in sector B than the instrumental sensitivity (1 nT), while in sector A it has a maximum of 2 nT (Table 1 and Fig. 6). In this second case, however, it is possible to observe more high-frequency noise in the magnetogram registered at the ground station coming from the electrical activity of nearby lighthouse, and higher in 1994JD76 than in 1994JD83.

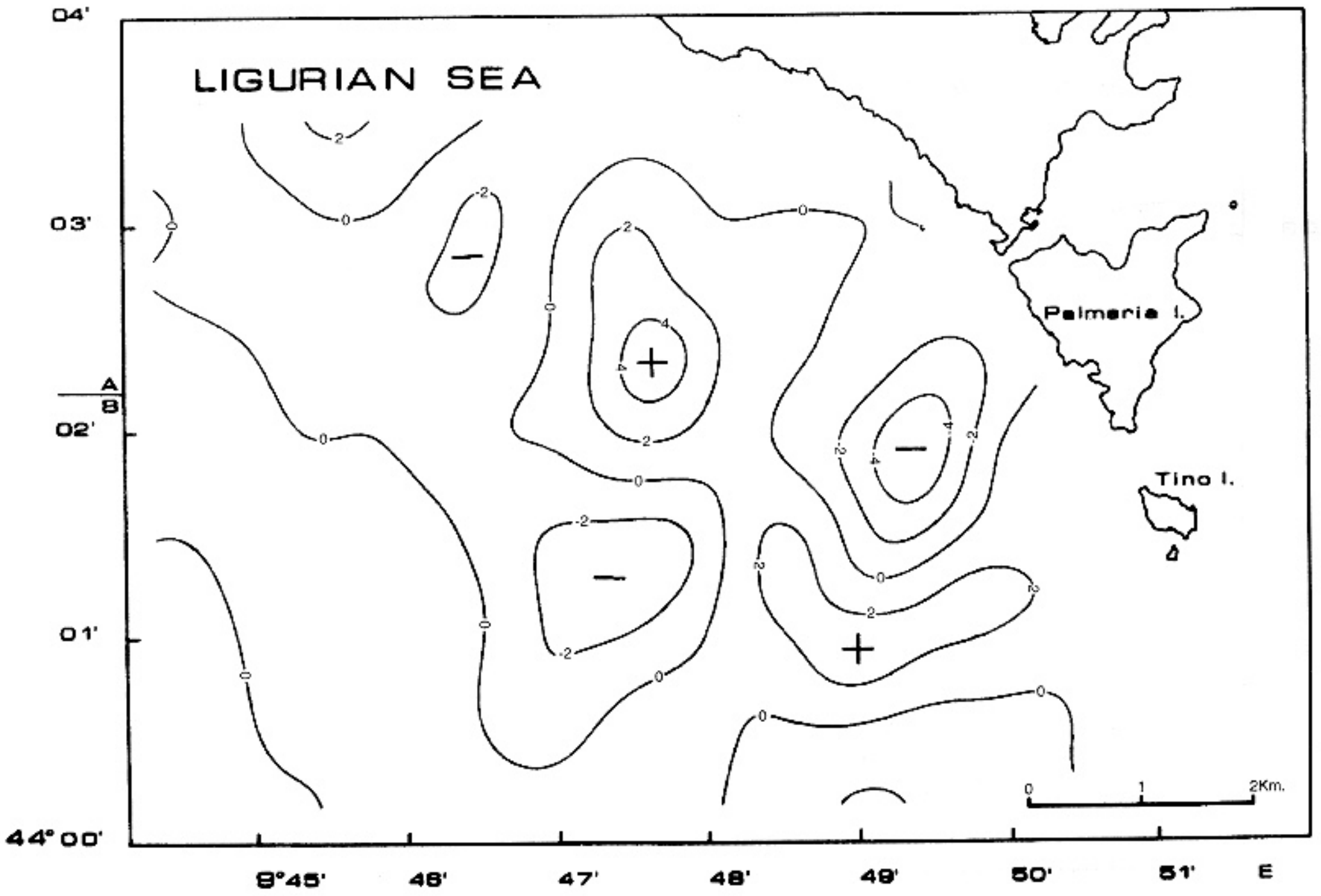

Fig. 11 - Spectral anomaly intensity field (SAF); high-pass filter: 1.8 km (minus mean value). Band of the represented harmonic components: 0.5 ÷ 1.8 km. C.I. = 2nT.

4. Geophysical elaboration and results

The time-reduced map of the total intensity geomagnetic field (Briggs, 1974) in the marine study area, free of the time variation component, shows a geometric structure which is different from that shown in the observed field map. The field variation zone, which in the observed map was directed along the geographic parallel, is now distributed over an area of magnetic high, including an absolute maximum and a relative maximum, along an axis approximately oriented NNW-SSE for a distance of about 6500 m (Fig. 7). The intensity of the two maxima are 46255 nT and 46254 nT. On both sides of this high are areas of low intensity which develop along an ENE-WSW axis, with minima of 46243 nT to the WSW, and of 46241 nT to the ENE. In these areas, the variation of the geomagnetic field total intensity is 14 nT. This variation is connected to space magnetic non-homogeneities, which the wavelenght characteristics suggest to be due to surface magnetic sources.

However, interpretation of a total field map is not straightforward, because the dipole structure of the surface geomagnetic field does not vary according to the geomagnetic latitude. Reduction to the pole (Arkani-Hamed, 1988; Telford et al., 1990) is one of the most important numerical tools used to simplify total field maps, and then to facilitate their interpretation. The reduction turns the local inclination of the geomagnetic field to the vertical direction.

The reduction was carried out using a field orientation factor based on the INGRF (Baranov,

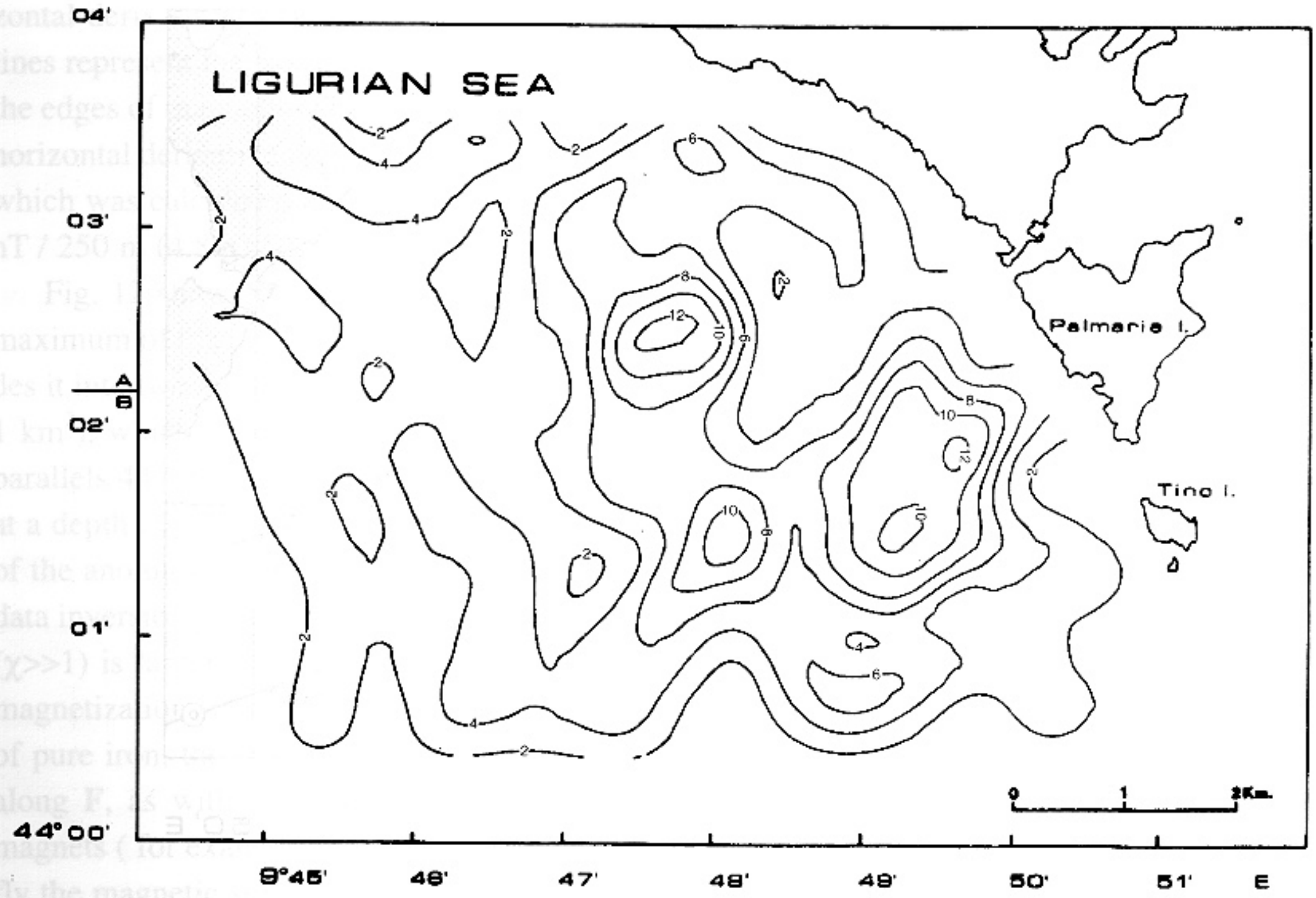

Fig. 12 - Horizontal derivative map. Absolute value of the field average increase unit: 4.8 nT/km. C.I. = 2 units. Matrix of calculus: 5.750 km x 8.750 km; calculation square grid side: 0.250 km.

1957; Spector and Grant, 1985; Silva, 1986). At latitude 44° 02' N and longitude 09° 48' E, and time March 1994, this reference field has computed declination angle *D* 7'.20 (+) and computed inclination angle *I* = 60° 12' (Meloni et al., 1994). The reduced-to-the-pole map (Fig. 8) confirms the indications of the rime-reduced map, and shows that the geomagnetic field isolines in general have a direction near to the meridian than to the parallel. In order to divide the two groups of variations and to produce a background geomagnetic signal map and an anomaly map, we chose the bidimensional frequency filtering technique rather than the IGRF (Langel, 1991) or DGRF or normal field residue procedures. In fact, in detailed surveys of low latidude and longitude extension, these reference fields, which are specifically for larger areas, cannot clearly separate the frequency categories. The technique we used to create our local reference field is that described by Schouten and McCamy (1972), Lowes (1974), and Kanasewich (1975).

The amplitude spectrum of the reduced geomagnetic field is shown in Fig. 9. There is clear difference among the harmonic components at the 4th order, equivalent to a cut-off wavelength of 1800 m. We obtained our spectral reference field (SRF) (Bullard, 1967; Slotweg, 1978; Faggioni and Carmisciano, 1993) by applying a LP filtering at this wavelength (Fig. 10). The local anomaly field 1.8 km HP SAF (spectral anomaly field; Oppenheim, 1968) was then deduced by deconvolution from the time-reduced field of the 1.8 km LP SRF as the short-wavelength field (Fig. 11). This anomaly field runs from -5 nT to 5 nT. Thus, the total intensity of the geomagnetic anomaly field, which can be linked to surface sources, is of 10 nT. The magnetic ano-

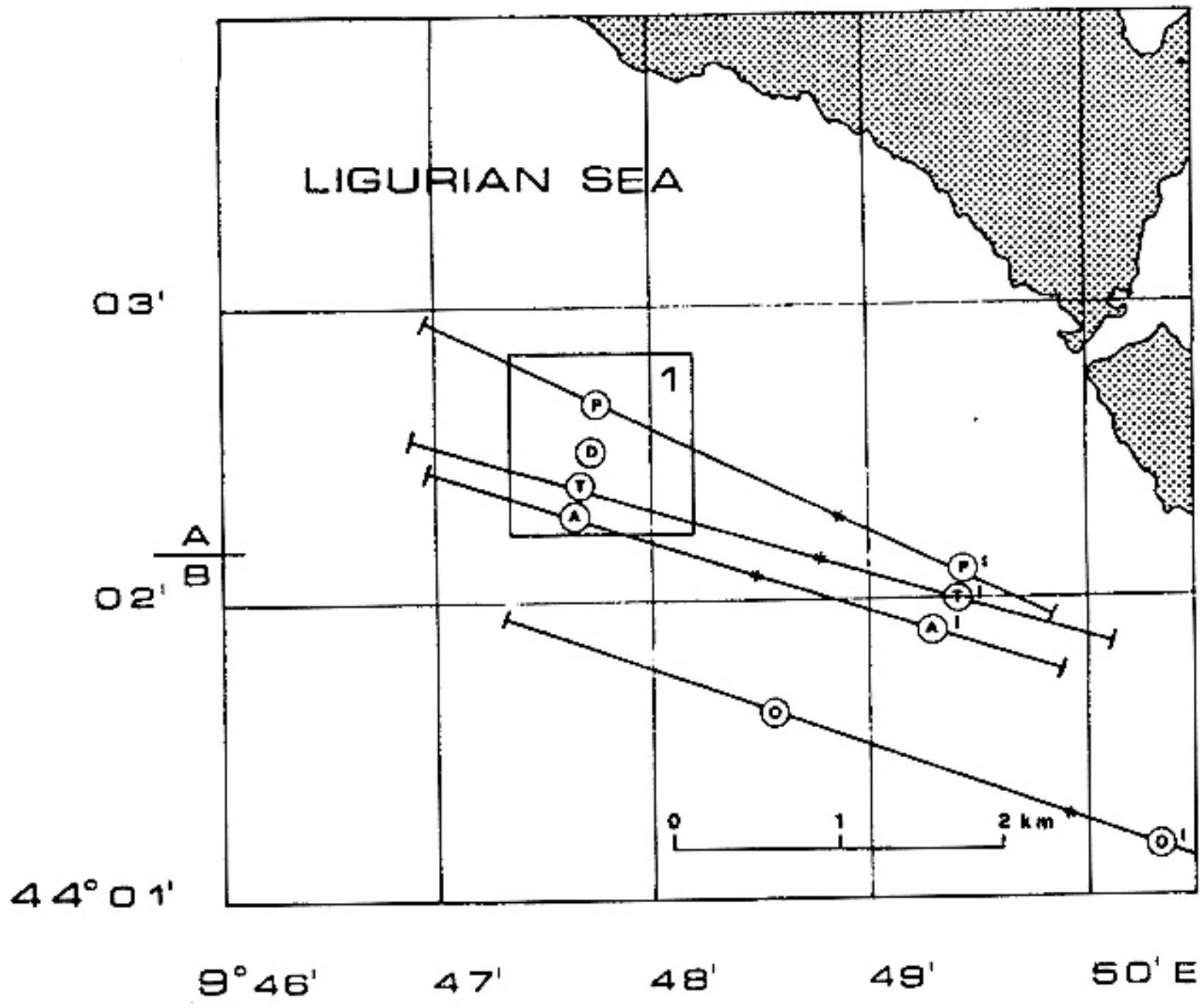

Fig. 13 - 1 - Metal body lies area. Board parallels 44° 02' 14" N - 44° 02' 50" N, meridians 9° 47' 20" E - 9° 48' 10" E. Orientations of measured and elaborated geomagnetic variations axes of geomagnetic F fields: O - O' measured field (Maximum of field = 46265 nT (O), minimum = 46253 nT (O') reference field value, flex point (star) and segment ends = 46258 nT); T - T' time reduced field (Maximum of field = 46255 nT (T), mininum = 46241 nT (T'), F variation reference field value, flex point (star) and segment ends = 46250 nT); P - P' polar (and time) reduced field (Maximum of field = 46257 nT (P), minimum = 46243 nT (P'), flex point (star) and segment ends = 46249 nT). A' axis of spectral HP 1.8 km time reduced anomaly field (A = +5 nT, A' = -5 nT, flex point (star) and segment ends = 0). D - horizontal derivative time reduced field maximum value (62.4 nT/km).

maly map provides a direct assessment of the intensity and space distribution of the field related to possible surface magnetic sources: it is therefore a quality instrument for their location (Faggioni et al., 1991). In our case, an anomaly between the parallels 44° 00' 40"N and 44° 03' 20"N, and the meridians 9° 47' 00"E and 9° 50' 00"E is now evident. This area shows two different dipole anomaly subareas, characterized by an approximate wavelength of 3500 m, with the major axis direction ESE-WNW, and different intensities and polarities. Tha main anomaly has an intensity of 10 nT and a positive polarity to the WNW; the secondary anomaly, further offshore than first, has a positive ESE polarity and an intensity of about 6 nT (Fig. 11).

A useful procedure for a better positioning of a source with respect to the fields is to determine the abrupt lateral changes in magnetization, which indicate the presence of magnetized bodies. This lateral behaviour of the field is particularly intense when ferromagnetic material is present. The artificial anomalies produced by surface metal objects are in fact characterized by high intensity and wavelength, *i.e.*, they have a high horizontal and vertical gradient. The hori-

zontal derivative field map (Fig. 12) best evidences this phenomenon. In this map the contour lines represent the maximum horizontal gradient of the magnetic anomaly field that may overlie the edges of magnetic bodies (Blakely and Simpson, 1986). The numeric values, indicated on the horizontal derivative map, are proportional to the absolute value of the mean horizontal gradient, which was calculated on the numeric matrix for the entire study area, and assessed at about 1.2 nT / 250 m (4.8 nT/km).

Fig. 12 shows two horizontal high-derivative areas which correspond to the minimum and maximum of the main anomaly. This reduces the area of major interest to about 12 km^2 and divides it into two subareas in which to search for the surface magnetic sources. The first subarea (~ 1 km^2), which is better defined and has an intense lateral field variation, extends between the parallels 44° 02' 14"N and 44° 02' 50"N, and the meridians 9° 47' 20"E and 9° 48'10"E. Here, at a depth of about 30 m, lies a body, which is the probable source of the anomaly. Knowledge of the anomaly does not, however, allow a reconstruction of the magnetic source or a coherent data inversion process. The anomaly field generated by a body with high magnetic susceptibility ($\chi>>1$) is largely sensitive to its shape, because the inducing field is screened by the induced magnetization (Landau and Lifsits, 1969). If we assume that $\chi = 4\pi \times 10^3$ (SI), which is typical of pure iron, the observed anomaly is as consistent with a linear dipole of only 25 kg aligned along **F**, as with a massive sphere of 100 t. Moreover, the possible presence of permanent magnets (for example in the ships engine and in the axes of the propeller) could strongly modify the magnetic signature. However, considering the massive linear iron elements contained in a ship, the probable misalignement of this magnetic source with the inducing field, and the reduction of χ due to iron oxidation, we can conclude that the observed anomaly is consistent with the presence of a wreck of several tons, like the object subsequently revealed by submarine exploration. The presence of this body in one of the high-derivative areas provides a model correspondence between an anomaly source and the geometric structure of the goemagnetic field (figure 12). For example, it can be assumed that similar situations also exist in the second less defined but equally intense subarea, which stretches between the parallels 44° 01'10"N and 44° 02'45"N, and the meridians 9° 48'50"E and 9°50'15"E. For the first subarea synthetic model (Fig. 13) we drew the axes of the measured field variations (O-O') and of the time (T-T') and polar (P-P') reduced field variations; and the axis of the spectral anomaly field (A-A') and the position of maximum derivative point (D). We note that the points representing the maximum of the time and polar reduced field (T, P,) and the maximum of the anomaly (A) are in good correspondence with the area of the iron sources. Also, the horizontal derivative field maximum (D) is the best geometric reference for this area. On the contrary, the maximum value of the geomagnetic measured field (O) is very far from the wreck area. The correspondence between the reduced fields (especially the derivative field) and the artificial metal source allows us to limit the area for the undersea search.

5. Conclusions

The high definition study of a geomagnetic field structure involves two fundamental techni-

cal problems: the high detailed positioning of the measurement points and the correct estimation of the geomagnetic time variation. In our case, the first problem was resolved by means of a ship's position microwave station network, and by the use of a low magnetic noise vessel permitting the use of a short drag rope (< 50 m). The second problem was solved by using the magnetograms from the experimental observatory on the Isle of Tino.

The crossover error observed during the survey was assumed to derive only from the time variation of the field between the first and the second measurements of each cross point. Deconvolution of the time signal recorded by the geomagnetic station from the signal from the field measurements, produced a time-reduced field map which we demonstrated to be virtually free of any crossover error.

The spectral analysis then provide a complete outline of the wavelengths described by our survey. Thanks to this mathematical tool, we were able to define a local reference field which describes the largest wavelengths in the investigated area. This reference field, LP 1.8 km SRF, obtained with an LP filter of such wavelength was frequency deconvolved from the values of the time-reduced field and produced our **HP** 1.8 km SAF spectral anomaly field.

Knowledge of the position and structure of the anomalies, their reduction to the pole and, above all, the analysis of the horizontal derivative map of the anomaly field, which is directly related to the magnetization lateral variations, enabled us to locate the area where, at a depth of 35 m, a small wreck lies. It also enabled us to reduce the area for a submarine search to those regions which, in the geomagnetic maps, show the same geometric characteristics.

Without the numeric procedures used on the gathered data set, the position of the artificial source was not obtainable, because its effect is hidden by the geomagnetic field time variations and by the geomagnetic local field.

Acknoledgements. To the memory of Ing. Alberto Gubellini, Professor of Topography at the Università di Bologna and Antarctic explorer in the Programma Nazionale Ricerche in Antartide.
The authors wish to thank Iginio Marson of the Università di Trieste, Antonio Meloni of the Istituto Nazionale di Geofisica and Raffaello Carrara of our Institute for their suggestions and critical review of the manuscript. The authors also thank the following for their scientific, naval, technical and logistic support of the HDR Med Sea 94 Project: Istituto Nazionale di Geofisica, Roma (Italy), Marina Militare Italiana, Comando in Capo Alto Tirreno, La Spezia (Italy) and Istituto Idrografico, Genova (Italy), Whitehead Alenia Sistemi Subacquei, Livorno (Italy). We are particularly indebted to Paolo Mancini CV (AN) Italian Navy, Naval operations Coordinator for our Institute, for his support and for all the useful scientific discussions on the results of this research. We finally acknowledge for their technical support: Lucia Rossi, Giorgio Ginesi, Paolo Marin, Monica Mura, and everyone who contributed to the measurement operations.

References

Arkani-Hamed J.; 1988: *Differential reduction to the pole of regional magnetic anomalies.* Geophysics, **53**, 1592-1600.

Baranov V., 1957: *A New Method for Interpretation of Aeromagnetic Maps: Pseudo-Gravimetric Anomalies.* Geophysics. **22**, 359-383.

Berti G., Cantini P., Carrara R., Faggioni O. and Pinna E.; 1991: *Misure di anomalie magnetiche artificiali.* In: Atti X Conv. Gr. Naz. Geof. Terra Solida, Esagrafica, Roma, pp. 809-814.

Blakely R. J. and Simpson R.W.; 1986: *Approximating Edges of Source Bodies from Magnetic or Gravity Anomalies.* Geophysics, **51**, 1494-1498.

Bott M. H. P. and Hutton M. A.; 1970: *A matrix method for interpreting oceanic magnetic anomalies.* Geophys. J. R. Astron. Soc., **20**, 149-157.

Bozzo E., Caneva G., Cattaneo M., Faggioni O. and Meloni A.; 1985: *Anomalie delle variazioni di origine lito-astenosferica nell'Italia nord-occidentale.* Atti IV Conv. Gr. Naz. Geof. Terra Solida, 911-923; Roma 29-31 Ottobre 1985.

Briggs I. C.; 1974: *Machine Countouring Using Minimum Curvature.* Geophysics, **39**, 39-48.

Boulard E. C.; 1976: *Removal of trend from magnetic surveys.* Earth Planet. Sci. Lett., **2**, 293-300.

Cooley J. W. and Tukey J. M.; 1965: *An algorithm for the machine calculation of complex Fourie series.* Math. Compt., **91**, 297-301.

De Santis A.; 1993: *Tempeste, sottotempeste, e baie magnetiche.* Annali di Geofisica, **36**, Suppl. N 5-6.

De Vuyst A. and De Meyer F.; 1973: *Spectral analysis of geomagnetic data from one station (Dourbes 1960-1970).* Institut Royal Meteorologique de Belgique; Publ., **A**, n° **80**, 32.

Faggioni O. and Carmisiciano C.; 1993: *LP 30 km SRF of Alto Tirreno sea map.* Ist. di Misure e Sistemi Geofisici Integrati - La Spezia - Internal Report. (Not Classified).

Faggioni O., Carmisciano C., Carrara R. and Pinna E.; 1993: *Sistema automatico di misura delle variazioni del campo geomagnetico per lunghi periodi di osservzione.* In: Atti XII Conv. Gr. Naz. Geof. Terra Solida, Esagrafica, Roma, pp. 885-892.

Faggioni O., Palangio P. and Pinna E.; 1991: *Osservatorio geomagnetico stazione baia Terra Nova (Antartide): Ricostruzone Sintetica del Magnetogramma 01.00(UT)GG1.88:12.00(UT)GG18.88.* In: Atti X Conv. Geof. Terra Solida, Esagrafica, Roma, pp. 687-706.

Faggioni O., Pinna E., Savelli C. and Schreider A.; 1995: *Geomagnetism and Age Study of Tyrrhenian Seamounths.* Geoph., Jour., Int., **123**, 915-930.

Guennoc P., Jonquet H. and Sibuet J.-C.; 1979: *Presentation d'une Carte Magnetique de l'Atlantique Nord-Est.* C. R. Acad. Sci. Pris, Ser. D, **288**, 1011-1013.

Hansen R.O. and Childs J.R.; 1987: *The Antactic Continental Marging Magnetic Gradiometer Data: Suppresion of Time Variations.* In: Cooper A. K. and Davey F. J. (eds), The Antarctic Continental Marging: Geology and Geophysics of the Western Ross Sea, CPCEMR Earth Science Series, Houston, Texas, V. **5B**, pp. 139-153.

Harrison C. G. A. and Carle H. M.; 1981: *Intermediate Wavelength Magnetic Anomalies Over Ocean Basins.* J. Geophys Res., **86**, 11,585-11,599.

Kanasewich E. R.; 1975: *Time Sequence Analysis in Geophysics.* The University of Alberta Press, Edmonton, Canada, 44-47.

Landau L. D. and Lifsits E. M.; 1969: *Electrodynamique des Milieux Continus.* Ed. Mir, Moscow, Russia.

Langel R. A.; 1991: *International Geomagnetic Reference Field. 1991 Revision.* J. Geomag. Geoelectr., **43**, 1007-1012.

Lowes F. J.; 1974: *Spatial Power Spectrum of the Main Geomagnetic Field, and Extrapolation to the Core.* Geophys. J. R. Astron. Soc., **36**, 717-730.

Meloni A,. Battelli O., De Santis A. and Dominici G.; 1994: *The 1990 magnetic repeat station survey and normal reference fields for Italy.* Annali di Geofisica, **37**, 949-967.

Meloni A., Molina, F. Palangio P., Taccetti Q. and De Santis A.; 1984: *Automatic Digital Recording of Geomagnetic Elements by Means of a Proton Precession Magnetometer.* Geoph. Surveys, **6**, 339-350.

Meloni A. and Palangio P.; 1988: *L'Automazione degli Osservatori Geomagnetici nell'Istituto Nazionale di Geofisica.* Atti II Conv. Geomagnetismo e Aeronomia, 429-446.

Oppenheim A. W., Schafer R. W. and Stockam T. G. Jr.; 1968: *Nonlinear Filtering of Multiplied and Convolved Signals*. Proc. IEEE **56 (8)**, 1264-1291.

Palangio P., Marchetti M. and Di Diego L.; 1991: *Rumore Elettromagnetico Prodotto dalle Ferrovie Elettrificate. Effetti sulle Misure Magnetotelluriche e Geomagnetiche*. In: Atti X Conv. Gr. Naz. Geof. Terra Solida, Esagrafica, Roma, pp.745-760.

Palangio P. and Romeo G.; 1988: *Stazione Magnetometrica da Impiegare in Ambiente Antartico*. In: Atti II Conv. Geomagnetismo e Aeronomia, Roma 18-20 Ottobre, pp. 417-428.

Reagan R. D. and Rodriguez P.; 1981: *An Overview of the External Magnetic Field with Regard to Magnetic Surveys*. Gophys. Surv., **4**, 255-297.

Roberts D. G., Jones M. T. and Hulter P. M.; 1985: *Magnetic Anomalies in the Northeast Atlantic*. Inst. Ocean. Sci. Rep., **207**, 9 pp + 2 Charts.

Roest W. R., Dañobeitia J. J., Verhoef J. and Collette B. J.; 1992: *Magnetic Anomalies in the Canary Basin and the Mesozoic Evolution of the Central North Atlantic*. Mar. Geophys. Res., **14**, 1-24.

Schouten H. and McCamy K.; 1972: *Filtering Marine Magnetic Anomalies*. J. Geophys. Res., **77**, 7089-7099.

Shaw P. R. and Cande S. C.; 1990: *High-Resolution Inversion for South Atlantic Plate Kinematics Using Joint Altimeter and Magnetic Anomaly Data*. J. Geophys. Res., **95**, 2625-2644.

Silva J. B. C.; 1986: *Reduction to the Pole as an Inverse Problem and its Application to Low-Latitude Anomalies*. Geophysics, **51**, 369-382.

Slootweg A. P.; 1978: *Computer Contouring with a Digital Filter*. Mar. Geophys. Res., **3**, 401-405.

Spector A. and Grant, F. S.; 1985: *Statistical Models for Interpreting Aeromagnetic Data*. Geophysics, **50**, 1951-1960.

Swan D. and Young, I. F.; 1978: *Crossover Differences as an Indicaiton of Survey Accuracy*. Mar. Geophys. Res., **3**, 393-400.

Talwani N., Windisch C. C. and Langseth M. G.; 1971: *Reykjanes Ridge Crest: a Detailed Geophysical Study*. J. Geophys. Res., **76**, 473-517.

Telford W. M., Geldard L. P. and Sheriff R. E.; 1990: *Applied Geophysics Second Edition*. Cambrige University Press - Cambrige, 108-113.

Twigt W., Slootweg A. P. and Colette B. J.; 1979: *Topography and Magnetic Analysis of an Area Southeast of the Azores (36° N, 23° W)*. Mar. Geophys. Res., **4**, 91-104.

Twig W., Verhoef J., Rohr K., Mulder Th. F. A. and Colette B. J.; 1983: *Magnetics and Gravity Over the Kane Fracture Zone in the Cretaceous Magnetic Quiet Zone (African Plate)*. Proc. Kon. Ned. Ak. Wet., series B, **86**, 181-210.

Verohef J., Colette B. J., Dañobeitia J. J., Roeser H. A. and Roest W. R.; 1991: *Magnetic Anomalies Off West-Africa (20-38° N)*. Mar. Geophys. Res., **13**, 81-103.

Verohef J., Colette B. J., Miles P., R., Searle R. C., Sibuet J. C. and Williams C. A.; 1986: *Magnetic Anomalies in the Northeast Atlantic Ocean (35°-50° N)*. Mar. Geophys. Res., **8**, 1-25.

Verhoef J. and Scholten R. D.; 1983: *Cross-Over Analysis of Marine Magnetic Anomalies*. Mar. Geophys. Res., **5**, 421-435.

Vogt P. R. and Avery; 1974: *Detailed Magnetic Surveys in the Northeast Atlantic and Labrador Sea*. J. Geophys. Res., **79**, 363-389.